



Optimisation of multiple W/O/W nanoemulsions for dermal delivery of aciclovir

Julia C. Schwarz^a, Victoria Klang^b, Sandra Karall^b, Denise Mahrhauser^b, Guenter P. Resch^c,
Claudia Valenta^{a,b,*}

^a University of Vienna, Research Platform “Characterisation of Drug Delivery Systems on Skin and Investigation of Involved Mechanisms”, Althanstraße 14, 1090 Vienna, Austria

^b University of Vienna, Department of Pharmaceutical Technology and Biopharmaceutics, Faculty of Life Sciences, Althanstraße 14, 1090 Vienna, Austria

^c IMP-IMBA-GMI Electron Microscopy Facility, Institute of Molecular Biotechnology, Dr. Bohr-Gasse 3, 1030 Vienna, Austria

ARTICLE INFO

Article history:

Received 23 August 2011
Received in revised form
25 November 2011
Accepted 25 November 2011
Available online 3 December 2011

Keywords:

Nanoemulsion
Reverse micelles
Phase inversion temperature method
Skin
Aciclovir
Cryo electron microscopy

ABSTRACT

In the present study multiple W/O/W nanoemulsions were optimised for the dermal application of the antiviral drug aciclovir. The phase inversion temperature method was employed to prepare the formulations without the input of high pressure. During formulation design the ethoxylated surfactants were varied and if possible partly replaced by natural sugar surfactants. Multiple nanoemulsions with mean droplet sizes around 100 nm and polydispersity indices below 0.1 were prepared. At room temperature, they exhibited excellent physicochemical stability over an observation period of 6 months. Furthermore, cryo electron microscopy gave an insight into the microstructure of the multiple nanoemulsions. Moreover, the formulations' interaction with skin was analysed by ATR-FTIR. In Franz-type diffusion cell and tape stripping experiments aciclovir showed satisfying skin permeation from the novel nanoemulsions.

© 2011 Elsevier B.V. All rights reserved.

1. Introduction

In recent years, a large number of studies has dealt with the optimisation of oil-in-water emulsions with particle sizes in the lower submicron range (Yilmaz and Borchert, 2005; Hoeller et al., 2009; Klang et al., 2011a). These systems, conveniently termed “nanoemulsions”, are aimed at topical drug delivery or cosmetic applications on skin (Klang et al., 2011b; Patravale and Mandawgade, 2008). To this end, lipophilic actives are incorporated into the respective oil phase. However, there is a surprising lack of data on nanoemulsions optimised for the delivery of hydrophilic drugs despite the fact that such skin-friendly systems might prove to be more appropriate for the delivery of hydrophilic drugs on sensitive skin than classical systems such as hydrogels or other ethanol-based formulations (Watkinson et al., 2009). A possible drawback of nanoemulsion systems might be the tendency of hydrophilic drugs to recrystallise within the aqueous phase during longer storage periods, especially at refrigerated storage. Such issues may be overcome by the development of a multiple emulsion system. This technique has recently been adapted to

submicron-sized emulsions by incorporating hydrophilic compounds into reverse micelles located within the dispersed phase of an O/W nanoemulsion (Anton et al., 2010; Vrignaud et al., 2011). These W/O/W nanoemulsions can be conveniently created by the phase inversion temperature (PIT) method.

The aim of the present study was to optimise this technique as well as the involved surfactants to create eudermic W/O/W nanoemulsions for the dermal delivery of the hydrophilic drug aciclovir. Since this method has only been patented recently to create reverse micelle-loaded lipid nanocarriers (Vrignaud et al., 2011), no data exist on the potential of these novel systems as dermal drug delivery vehicles. Thus, this study represents the first substantiated approach to systematically study the novel carrier system for dermal application. Franz-type diffusion cell and tape stripping experiments were performed to investigate the skin permeation behaviour of the developed formulations. Moreover, the interaction of the developed multiple nanoemulsions with the stratum corneum was investigated by ATR-FTIR studies. Both the type and the amount of surfactant for the droplet formation as well as for the preparation of reverse micelles was varied to identify the lowest possible surfactant concentration which would lead to W/O/W systems of satisfying droplet size, physicochemical stability and skin permeation. Since the PIT method for the development of W/O/W nanoemulsions requires comparatively large amounts of ethoxylated surfactants, the optimisation of this technique using biodegradable sucrose ester surfactants was among the primary

* Corresponding author at: University of Vienna, Department of Pharmaceutical Technology and Biopharmaceutics, Althanstraße 14, 1090 Vienna, Austria.
Tel.: +43 1 4277 55410; fax: +43 1 4277 9554.

E-mail address: claudia.valenta@univie.ac.at (C. Valenta).

interests of this study. Thus, the advantages and drawbacks of these compounds that were observed for the presented application are discussed in detail.

2. Materials and methods

2.1. Materials

Solutol HS 15 (polyoxyethylene-660-12-hydroxy stearate, HLB 14–16) was kindly donated by BASF, Germany. Ryoto sugar ester S-1670 with a HLB of 16 (75% sucrose stearate monoester) and S-270 with a HLB of 2 (10% sucrose stearate monoester) were a gift from Mitsubishi-Kagaku Foods Corporation, Japan. Miglyol 815 (neutral oil) was purchased from Dr. Temt Laboratories, Austria, and aciclovir from Fagron, Germany. Methanol for HPLC analysis and Span 80[®] (sorbitane monooleate, HLB 4) were obtained from Sigma Aldrich, Austria.

2.2. Methods

2.2.1. Nanoemulsion preparation

The preparation of W/O/W nanoemulsions was performed according to Anton et al. (2010) using the phase inversion temperature (PIT) method. The composition of the formulations is given in Table 1. A defined amount of the lipophilic surfactant above its critical micelle concentration (CMC) was poured into the oil phase. In case of aciclovir-loaded nanoemulsions, 1% of the active ingredient was added and stirred for two hours to ensure incorporation into the reverse micelles (formulations Sol-(Span)-ACV, Sol-(S270)-ACV, Sol-S1670-(S270)-ACV). For reasons of comparison, the same formulations were prepared without the two hours of stirring. In this case, we assumed that aciclovir was not incorporated into the reverse micelles (formulations Sol-(Span)-ACV-unencaps., Sol-(S270)-ACV-unencaps., Sol-S1670-(S270)-ACV-unencaps.). Subsequently, the hydrophilic surfactant, approximately 40% (w/w) of the water phase and sodiumchloride were mixed at room temperature. The temperature was slowly increased above the phase inversion temperature to about 85 °C. At this point, the reverse micelle-loaded oil phase was added dropwise. In a final step, the system was diluted abruptly with the remaining part of the distilled water at room temperature.

2.2.2. Physicochemical characterisation and stability

Mean droplet size (MDS), polydispersity index (PDI) and zeta potential (ZP) were determined with a Zeta Sizer Nano ZS (Malvern Instruments, United Kingdom). All samples were diluted 1:400 with 0.01 mM NaCl solution before the measurement. For the ZP measurements, the conductivity of the samples was kept constantly below 0.05 mS cm⁻¹. Moreover, the pH was determined for each formulation. In order to obtain information about the stability of the formulations, the above mentioned parameters were determined over a period of 6 months. The formulations were stored at room temperature (25 ± 2 °C, 60 ± 5% RH).

2.2.3. Cryo electron microscopy

Samples for cryo transmission electron microscopy (TEM) were frozen with a Leica EM GP immersion freezer (Leica Microsystems, Austria) according to Resch et al. (2011). The environmental chamber of the TEM was operated at 37 °C and 90% relative humidity. 4 µl of the specimen were diluted 1:10 (formulation A) or 1:3 (formulations B and C) with distilled water, pre-warmed to 37 °C and applied onto a glow discharged EM grid coated with a perforated Quantifoil R1.2/1.3 carbon film (Quantifoil, Germany). After 30 s, the suspension was blotted for 1.0 s with Whatman No. 1 filter paper using the instrument's blotting sensor and immediately plunged into liquid ethane just above its freezing point (−184 °C).

The vitrified specimens were visualised at liquid nitrogen temperature on a Tecnai F30 'Helium' (Polaris) cryo-TEM (FEI Company, Netherlands) operated at 300 kV. Low dose micrographs were acquired at nominal magnification of 31,000× at a defocus of −10.0 µm for high contrast and captured with a Gatan US4000 CCD camera.

2.2.4. In vitro skin studies

Franz-type diffusion cell and tape stripping experiments were performed as previously described in Schwarz et al. (2011). Porcine skin samples were stored in a freezer at −18 °C for a maximum of 6 months. For the Franz-cell experiments, dermatomed abdominal pig skin of 500 µm thickness was used as a model membrane. An infinite dose of 50 mg cm⁻² of formulation was applied onto the skin. Phosphate buffer (pH 7.4, 0.012 M) served as an acceptor medium. Samples were taken after 2, 4, 6 and 8 h. The aciclovir content in each sample was determined with HPLC analysis.

Tape stripping experiments were performed on full-thickness porcine ear skin. The hair was carefully removed by clipping. Subsequently, 5 mg cm⁻² of the formulation was applied. After a residence time of one hour, twenty tape strips were removed at a defined area and individually analysed for the amount of corneocytes by NIR (Klang et al., 2011b). The corresponding content of aciclovir was analysed by HPLC after extraction of the tape strips with methanol (Klang et al., 2011d, 2011c). The entire horny layer thickness was determined beforehand by removing the whole stratum corneum with up to 80 tape strips. This procedure was stopped when the limit of detection of the NIR densitometer was reached.

2.2.5. HPLC analysis

The quantitative analysis of aciclovir was carried out by HPLC (Perkin Elmer, Austria) using a UV diode array detector (235C). The wavelength of detection was set at 280 nm. A Nucleosil 1005 C18 column (250 mm × 4 mm, MachereyNagel, USA) plus precolumn (SS 8/4) was used for analysis. The mobile phase consisted of methanol/water (10/90) and was pumped through the system at a flow rate of 1 ml min⁻¹ (Hasanovic et al., 2010). The calibration curve ranged from 0.3 to 506 µg/ml.

2.2.6. ATR-FTIR spectroscopy

The effect of the developed W/O/W nanoemulsions on skin was also investigated by ATR-FTIR spectroscopy. Infrared spectra of impregnated porcine ear skin samples were obtained using a Tensor 27 FTIR instrument (Bruker Optics, Germany) with a Bio-ATR I tool and a photovoltaic MCT detector at the skin surface temperature of 32 °C. Porcine ear skin samples were treated as described in Hasanovic et al. (2011). For the measurements, the skin samples were placed on the ZnSe ATR crystal with the stratum corneum facing down. A weight of 100 g was placed on each sample to keep the intensity of the spectra constant. Data analysis was performed using the OPUS software version 5.5.

2.2.7. Statistical analysis

All results are mean values ± standard deviation of three or more experiments. The statistical analysis was performed using the student's *t*-test with *p* < 0.05 as level of significance (GraphPad Prism Software, USA).

3. Results and discussion

3.1. Nanoemulsion characterisation

In preliminary studies the lowest amount of surfactant required for nanoemulsification was determined. While blank nanoemulsions containing between 3% and 4.5% (w/w) of the hydrophilic surfactant Solutol HS15 exhibited particle sizes above 140 nm with

Table 1

Composition of the multiple W/O/W nanoemulsions [% (w/w)]. The reverse micelle forming surfactant is displayed in parentheses. Abbreviations: Sol (Solutol HS 15), Span (Span 80), ACV (aciclovir).

Formulation	Solutol HS15	S1670	Span 80	S270	Miglyol 812	NaCl	Aqua dest.	ACV
A								
Sol-(Span)	5.00	–	0.25	–	8.35	0.60	84.80	–
Sol-(Span)-ACV	5.00	–	0.25	–	8.35	0.60	84.80	1.00
Sol-(Span)-ACV-unencaps.	5.00	–	0.25	–	8.35	0.60	84.80	1.00
B								
Sol-(S270)	5.00	–	–	0.25	8.35	0.60	84.80	–
Sol-(S270)-ACV	5.00	–	–	0.25	8.35	0.60	84.80	1.00
Sol-(S270) ACV-unencaps.	5.00	–	–	0.25	8.35	0.60	84.80	1.00
C								
Sol-S1670-(S270)	4.30	0.70	–	0.25	8.35	0.60	84.80	–
Sol-S1670-(S270)-ACV	4.30	0.70	–	0.25	8.35	0.60	84.80	1.00
Sol-S1670-(S270)-ACV-unencaps.	4.30	0.70	–	0.25	8.35	0.60	84.80	1.00

polydispersity indices of 0.15 and higher, formulations with 5% (w/w) surfactant showed excellent physicochemical properties with a mean droplet size of about 105 nm and PDI values around 0.07 (Table 2, formulation A). Therefore, the content of hydrophilic surfactant was set at 5% (w/w). Subsequently, the lipophilic surfactant employed for the formation of reverse micelles was varied. To this end, Span 80 was replaced by the natural sugar surfactant S270. As a result even smaller particle sizes and lower PDI values were obtained (Table 2, formulation B). As a final step the nature of the hydrophilic surfactant was altered. Only polyethoxylated surfactants such as Solutol HS 15 show the characteristic temperature-dependent phase inversion behaviour which is necessary to form nanoemulsions by the PIT method (Anton et al., 2007). However, polyethoxylated surfactants are sometimes viewed critically regarding their skin compatibility (Bergh et al., 1998). Thus, we attempted to partially replace the ethoxylated surfactant by the biodegradable and eudermic surfactant sucrose stearate (Klang et al., 2011a). A combination of Solutol HS 15 and the sugar surfactant S1670 (13+2) was found to lead to satisfying results. A further reduction in mean droplet size and PDI values was observed (Table 2, formulation C). As expected, a complete replacement of Solutol HS 15 by S1670 was not feasible as the mean droplet size and the polydispersity index deteriorated to unacceptable values.

In summary, the nature of the lipophilic surfactant was important for the particle size distribution. The replacement of Span 80 by sucrose stearate S270 resulted in a decrease in the mean droplet size and PDI; the zeta potential and pH values remained almost identical. We can therefore recommend this optimisation strategy. In case of the hydrophilic surfactant, a decrease of mean droplet size was observed after a partial replacement of the polyethoxylated surfactant by the sugar surfactant S1670. However, the polydispersity index increased suggesting a more inhomogeneous droplet size distribution. Since the corresponding absolute zeta potential

value increased it may nevertheless be assumed that the overall stability might not be impaired. The value of a mixed hydrophilic surfactant film for this preparation method remains therefore to be investigated with further formulations.

The described formulations A, B and C were prepared both without drug and with aciclovir. The latter was encapsulated into reverse micelles. The successful incorporation into the reverse micelles was confirmed on one hand by visual inspection and on the other hand by the smaller droplet sizes and narrow size distributions as detected by dynamic light scattering (DLS). The prepared systems formed spontaneously without additional energy input and exhibited a uniform blueish translucent appearance. For reasons of comparison, formulations A, B and C were also prepared without encapsulating aciclovir into reverse micelles. In addition to their less homogeneous appearance, these formulations showed significantly higher particle sizes with larger standard deviations and more variable PDIs (Table 2 and Fig. 1b). Although all reverse micelle loaded formulations exhibited satisfying physicochemical properties, formulation B (Sol-(S270)) possessed the most favourable characteristics with a mean droplet size of about 100 nm and an excellent polydispersity index of about 0.09.

3.2. Physicochemical stability

In order to evaluate the stability of the multiple nanoemulsions, the discussed physicochemical parameters were monitored over a period of 6 months. The formulations exhibited excellent intermediate stability at room temperature. The values of all determined parameters showed no significant differences from the initial values given in Table 1 over the whole observation period ($P > 0.05$ in all cases). As indicated in Fig. 1a, the mean droplet sizes of formulation A, B and C remained largely constant. Neither the PDI nor the ZP or pH values varied significantly over the whole

Table 2

Physicochemical parameters of the formulations. Abbreviations: MDS, mean droplet size; PDI, polydispersity index; ZP, zeta potential.

formulation	MDS (nm)	PDI	ZP [mV]	pH
A				
Sol-(Span)	104.54 ± 3.53	0.070 ± 0.007	−6.19 ± 5.50	6.1 ± 0.2
Sol-(Span)-ACV	108.12 ± 0.26	0.189 ± 0.131	−15.88 ± 0.59	6.3 ± 0.1
Sol-(Span)-ACV-unencaps	125.29 ± 24.25	0.236 ± 0.231	−13.24 ± 1.98	6.1 ± 0.2
B				
Sol-(S270)	88.73 ± 3.35	0.064 ± 0.011	−15.07 ± 1.80	6.0 ± 0.1
Sol-(S270)-ACV	99.02 ± 2.74	0.091 ± 0.024	−13.17 ± 1.59	6.1 ± 0.1
Sol-(S270)-ACV-unencaps	114.51 ± 11.03	0.270 ± 0.169	−10.80 ± 3.81	6.1 ± 0.0
C				
Sol-S1670-(S270)	63.34 ± 0.19	0.080 ± 0.006	−20.30 ± 4.10	5.9 ± 0.0
Sol-S1670-(S270)-ACV	74.61 ± 4.40	0.283 ± 0.110	−20.60 ± 2.70	5.8 ± 0.0
Sol-S1670-(S270)-ACV-unencaps	122.26 ± 56.34	0.295 ± 0.136	−29.70 ± 6.00	5.9 ± 0.1

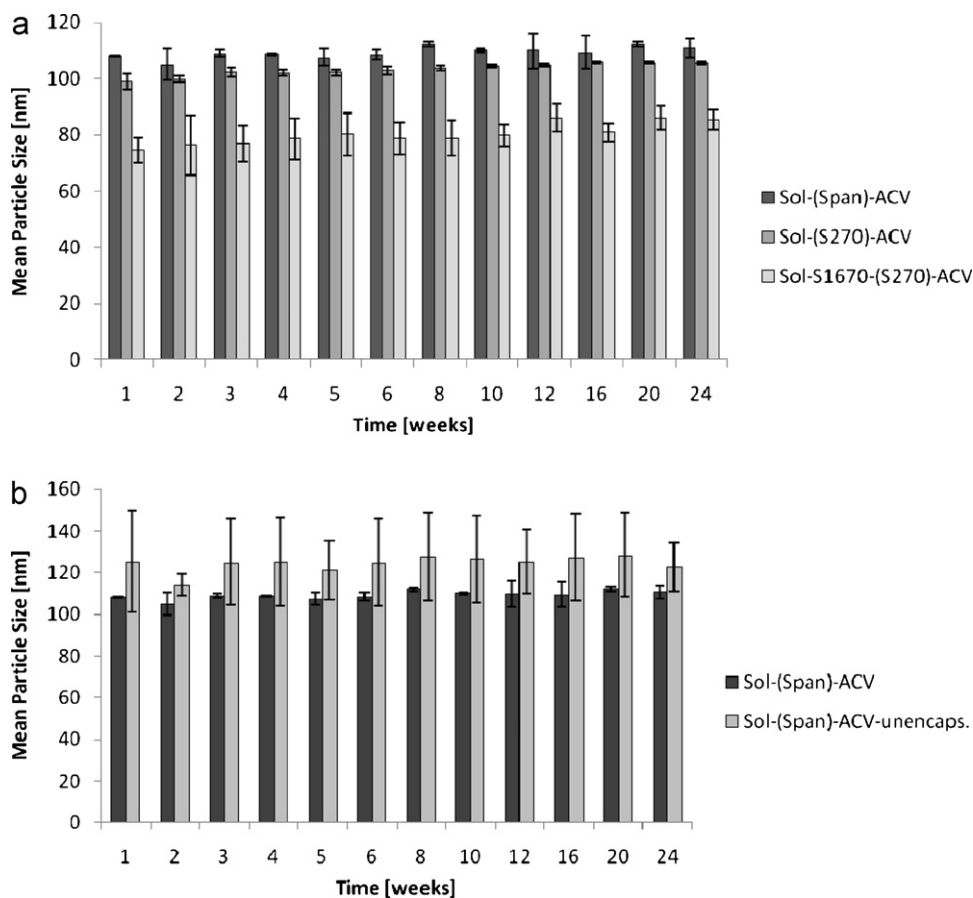


Fig. 1. (a) Mean droplet size of investigated formulations with aciclovir as determined over 24 weeks. Formulations A: Sol-(Span)-ACV (dark grey); B: Sol-(S270)-ACV (medium grey); C: Sol-S1670-(S270)-ACV (light grey). (b) Mean droplet size of investigated formulations with aciclovir as determined over 24 weeks. Formulations A: Sol-(Span)-ACV (dark grey); A-unencaps: Sol-(Span)-ACV-unencaps (light grey).

observation period ($P > 0.05$, respectively). Moreover, an observation of the physicochemical stability parameters of the nanoemulsions with aciclovir encapsulated into reverse micelles compared to those of the nanoemulsions with unencapsulated aciclovir showed significantly better results for the reverse micelle loaded formulations ($P < 0.05$, respectively; Fig. 1b). The formulations with aciclovir encapsulated in reverse micelles possessed significantly smaller mean droplet sizes with narrower size distribution which remained constant over 6 months ($P < 0.05$).

3.3. Cryo electron microscopy

Cryo TEM studies were conducted to gain a deeper insight into the microstructure of the nanoemulsions (Fig. 2). As can be clearly seen in the obtained images, the oil droplets were uniformly dispersed in the surrounding bulk water phase. However, the reverse micelle structures inside the oil droplets were too small to be visualised with this technique. Furthermore, formulation C showed the most smoothly shaped oil droplets. This might be due to the employment of sucrose stearate in the hydrophilic surfactant mixture with Solutol HS 15. As generally known, mixed surfactant films are usually more flexible and thus more suitable to form emulsified oil droplets of spherical shape (Trotta et al., 2002). In addition, the microscopic investigations served to confirm the DLS data. Since DLS alone exhibits certain limitations for the analysis of nanoemulsion droplet size (Klang et al., 2011e), an additional technique such as cryo electron microscopy is strongly recommended. Indeed, the mean droplet sizes of all three formulations as determined by DLS

were in good agreement with the microscopically observed droplet sizes.

3.4. In vitro skin studies

The skin permeation experiments using Franz-type diffusion cells revealed that formulation A-ACV and A-ACV-unencaps. led to very similar permeation rates ($P > 0.05$). In addition, the flux of aciclovir from both nanoemulsions was approximately 1.3-times higher than the flux of aciclovir from an aqueous solution ($P < 0.05$, respectively; Fig. 3a). The latter finding was not surprising since formulation A-ACV and A-ACV-unencaps. contained the same amount of surfactants. Most surfactants can generally be considered as permeation enhancers. Thus, the skin permeation of the active compounds from a formulation will most likely be higher than the drug permeation from an aqueous solution without any additives. Subsequently, the three final W/O/W nanoemulsions were compared regarding their skin diffusion potential. All of them showed excellent skin permeation properties. Between 70% and 80% of the incorporated drug had permeated through the skin after 8 h. Formulation B-ACV showed a slightly superior drug flux of 59.21 ± 2.89 in comparison to formulation A-ACV with a flux of 56.68 ± 3.59 and formulation C-ACV with a flux of 55 ± 4.70 (Fig. 3b). However, these differences did not reach statistical significance ($P > 0.05$, respectively).

The observed trends were confirmed in tape stripping experiments on porcine ear skin. Fig. 4 shows a representative skin penetration profile of aciclovir from formulation A-ACV. In case of formulation A-ACV and B-ACV, skin penetration depths of about

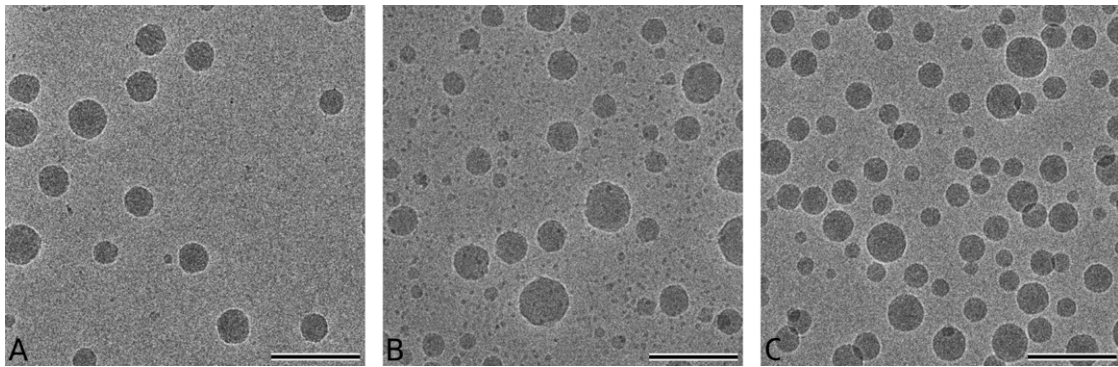


Fig. 2. Cryo electron microscopic images of formulations A: Sol-(Span), B: Sol-(S270) and C: Sol-S1670-(S270). The scale bars represent 200 nm.

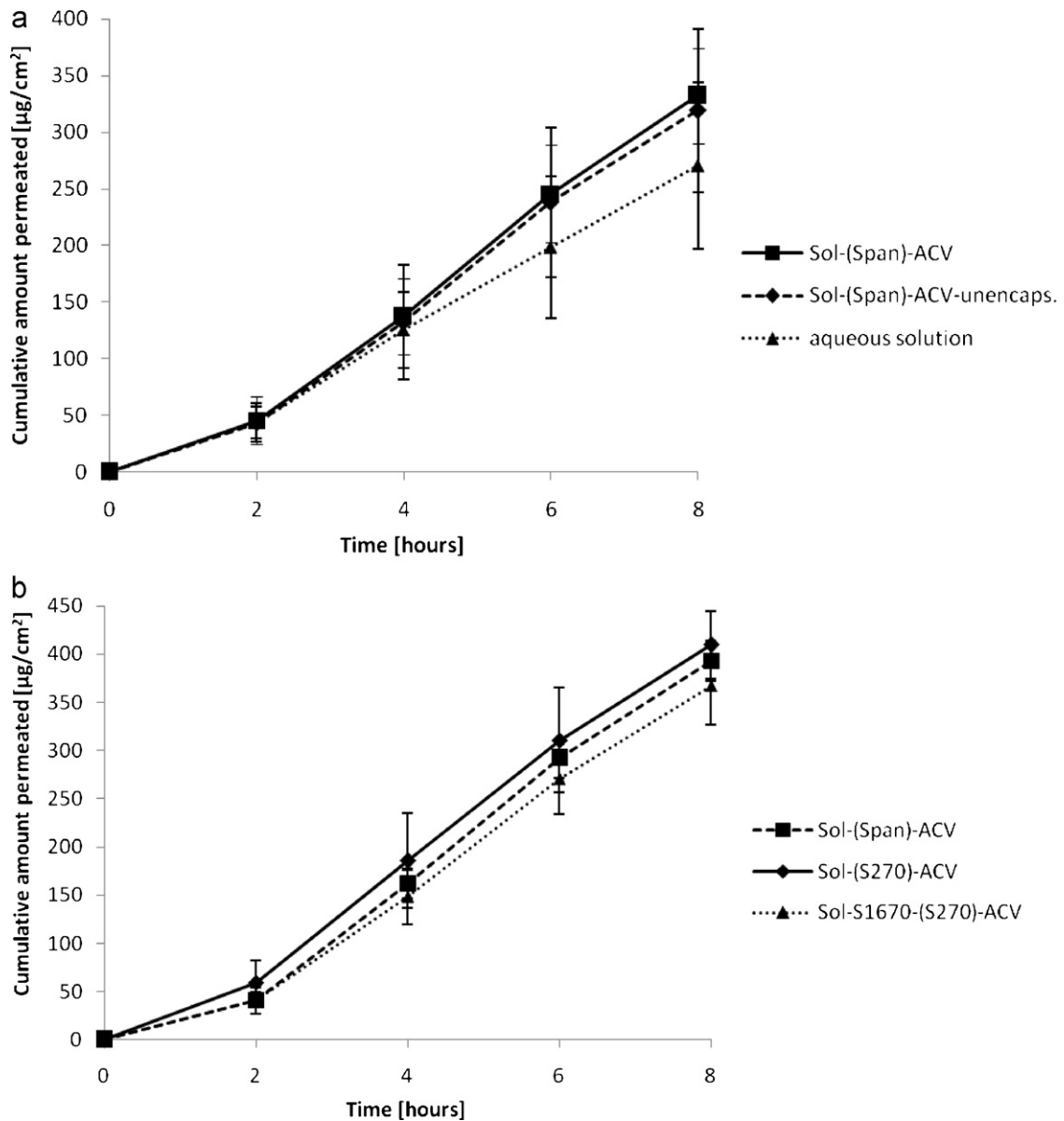


Fig. 3. (a) Skin permeation of aciclovir from an aqueous solution of ACV ($\cdots\blacktriangle\cdots$) and from formulations A: Sol-(Span)-ACV ($-\blacksquare-$); Sol-(Span)-ACV-unencaps. ($-\blacklozenge-$). (b) Skin permeation of aciclovir from formulations A: Sol-(Span)-ACV ($-\blacksquare-$); B: Sol-(S270)-ACV ($-\blacklozenge-$); C: Sol-S1670-(S270)-ACV ($\cdots\blacktriangle\cdots$).

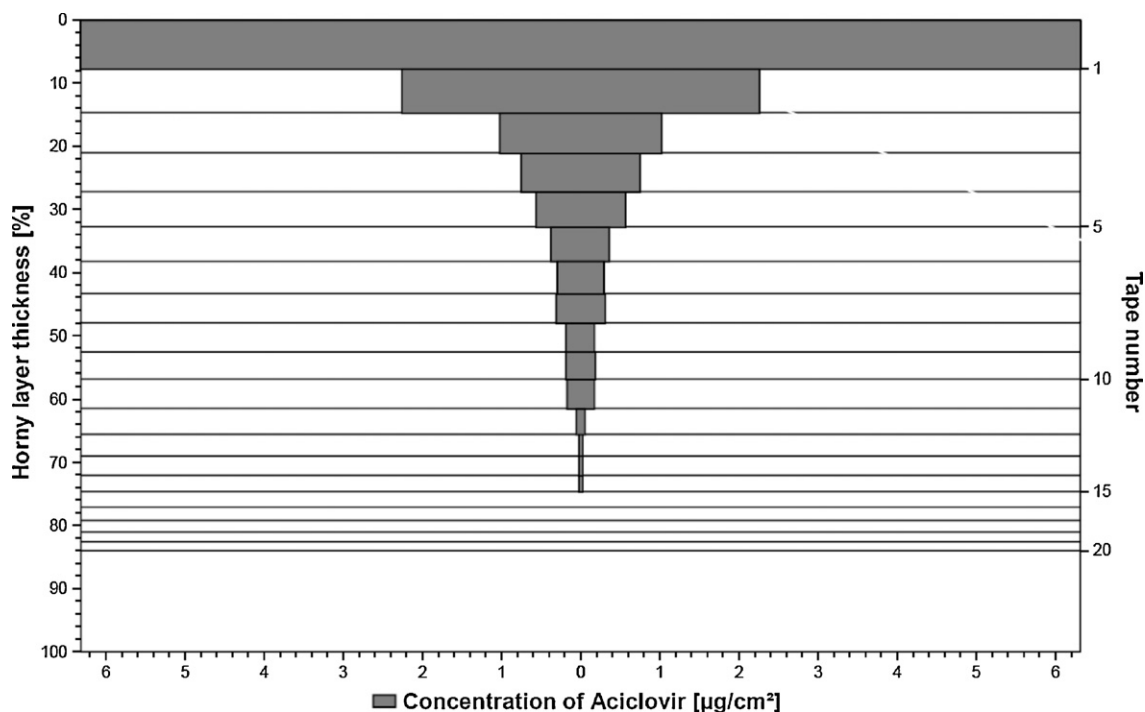


Fig. 4. Representative skin penetration profile of aciclovir from formulation A: Sol-(Span)-ACV.

75% of the entire stratum corneum thickness were reached. In case of formulation C-ACV, the penetration depth of aciclovir was found to be lower. Again, as for the Franz cell studies, the observed differences in penetration depth did not reach statistically significant levels ($P > 0.05$, respectively).

3.5. ATR-FTIR

A major focus of this study was the effect of the multiple nanoemulsions on the skin and in particular on the stratum corneum. While tape stripping and Franz-type diffusion cell

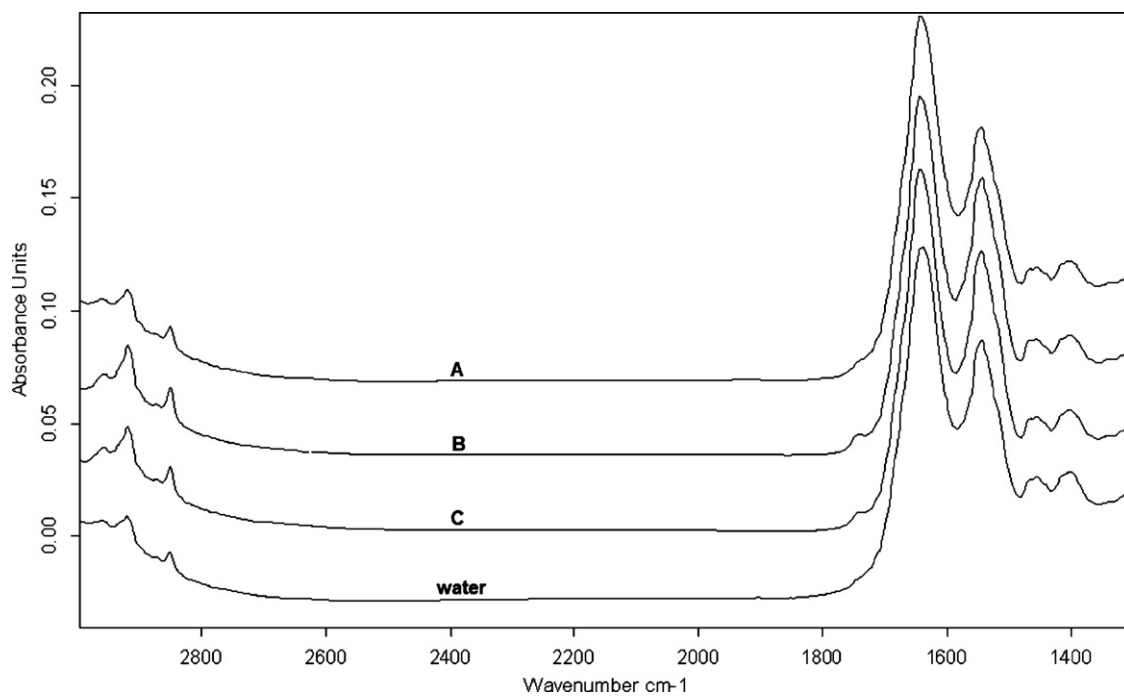


Fig. 5. ATR-FTIR spectra of porcine ear skin after incubation for 2 h with the investigated formulations A: Sol-(Span), B: Sol-(S270) and C: Sol-S1670-(S270) in comparison to porcine ear skin incubated with water.

experiments were employed to elucidate the drug delivery from the developed systems into and through the skin, ATR-FTIR spectroscopy was used to analyse the interaction between the formulations and the stratum corneum on a molecular level. Spectra of porcine ear skin incubated with the formulations were compared to those of porcine ear skin incubated with water. The following bands were recorded: CH₂ asymmetric (2920 cm⁻¹) and symmetric stretching vibration (2850 cm⁻¹), amide I (C=O) vibration (1640 cm⁻¹) and amide II (C–N) vibration (1540 cm⁻¹) and the CH₂ scissoring mode (between 1470 and 1460 cm⁻¹). These bands are caused by the intercellular lipids and keratin inside the corneocytes of the skin and correlate well with values found in the literature (Hasanovic et al., 2011; Obata et al., 2010; Rodríguez et al., 2010). In Fig. 5, a spectrum of pig ear skin incubated with water is presented in comparison with spectra of porcine ear samples incubated with formulation A, B and C, respectively. Although most bands were observed to be identical, there was a significant shift of the amide I band from 1639 cm⁻¹ after incubation with water to 1643 cm⁻¹. This shift was observed for all three formulations and may indicate a change in the secondary structure of keratin. It may be assumed that a conformational change from mostly α -helical to a higher content of β -sheet occurs, possibly resulting in a less tightly packed structure (He et al., 2009; Babita et al., 2006).

4. Conclusion

The optimised W/O/W nanoemulsions are well suited for the dermal delivery of aciclovir. A satisfying skin penetration potential of aciclovir from the formulations was observed in different experiments. The employed PIT method allowed for a simple and rapid preparation of nanoemulsions with excellent physicochemical properties which remained constant upon storage during the whole observation period. Cryo TEM confirmed mean droplet sizes of around 100 nm as found by dynamic light scattering. Further studies shall examine the antiviral properties of the developed formulations in vitro and in vivo.

Acknowledgments

The authors would like to thank the research platform “Characterisation of drug delivery systems on skin and investigation of involved mechanisms”, University of Vienna, Austria, for financing this project. The work of G.P.R. is funded by the City of Vienna/Centre for Innovation and Technology via the Spot of Excellence Grant “Centre of Molecular and Cellular Nanostructures”. Moreover, we would like to express our gratitude to J. Lademann for valuable assistance with the tape stripping technique.

References

Anton, N., Gayet, P., Benoit, J.P., Saulnier, P., 2007. Nano-emulsions and nanocapsules by the PIT method: an investigation on the role of the temperature cycling on the emulsion phase inversion. *Int. J. Pharm.* 344, 44–52.

- Anton, N., Mojzisova, H., Porcher, E., Benoit, J.P., Saulnier, P., 2010. Reverse micelle-loaded lipid nano-emulsions: new technology for nano-encapsulation of hydrophilic materials. *Int. J. Pharm.* 398, 204–209.
- Babita, K., Kumar, V., Rana, V., Jain, S., Tiwary, A.K., 2006. Thermotropic and spectroscopic behaviour of skin: relationship with percutaneous permeation enhancement. *Curr. Drug Deliv.* 3, 95–113.
- Bergh, M., Shao, L.P., Hagelthorn, G., Gaefvert, E., Nilsson, J.L.G., Karlberg, A.T., 1998. Contact allergens from surfactants. Atmospheric oxidation of polyoxyethylene alcohols, formation of ethoxylated aldehydes, and their allergenic activity. *J. Pharm. Sci.* 87, 276–282.
- Hasanovic, A., Hollick, C., Fischinger, K., Valenta, C., 2010. Improvement in physicochemical parameters of DPPC liposomes and increase in skin permeation of aciclovir and minoxidil by the addition of cationic polymers. *Eur. J. Pharm. Biopharm.* 75, 148–153.
- Hasanovic, A., Winkler, R., Resch, G.P., Valenta, C., 2011. Modification of the conformational skin structure by treatment with liposomal formulations and its correlation to the penetration depth of aciclovir. *Eur. J. Pharm. Biopharm.* (Feb 15): Epub ahead of print.
- He, W., Guo, X., Xiao, L., Feng, M., 2009. Study on the mechanisms of chitosan and its derivatives used as transdermal penetration enhancers. *Int. J. Pharm.* 382, 234–243.
- Hoeller, S., Sperger, A., Valenta, C., 2009. Lecithin based nanoemulsions: a comparative study of the influence of non-ionic surfactants and the cationic phytosphingosine on physicochemical behaviour and skin permeation. *Int. J. Pharm.* 370, 181–186.
- Klang, V., Matsko, N., Raupach, K., El-Hagin, N., Valenta, C., 2011a. Development of sucrose stearate-based nanoemulsions and optimisation through gammacyclodextrin. *Eur. J. Pharm. Biopharm.* 79, 58–67.
- Klang, V., Valenta, C., 2011b. Lecithin-based nanoemulsions. *J. Drug Deliv. Sci. Technol.* 21, 55–76.
- Klang, V., Schwarz, J.C., Hartl, A., Valenta, C., 2011c. Facilitating in vitro tape stripping: application of infrared densitometry for quantification of porcine stratum corneum proteins. *Skin Pharmacol. Physiol.* 24, 256–268.
- Klang, V., Schwarz, J.C., Lenobel, B., Nadj, M., Hartl, A., Auböck, J., Wolzt, M., Valenta, C. In vitro vs in vivo tape stripping: validation of the porcine ear model and penetration assessment of novel sucrose stearate emulsions. *Eur. J. Pharm. Biopharm.*, 2011 Nov. 22 [Epub ahead of print].
- Klang, V., Matsko, N.B., Valenta, C., Hofer, F., 2011e. Electron microscopy of nanoemulsions: an essential tool for characterisation and stability assessment. *Micron* (July 29): Epub ahead of print.
- Obata, Y., Utsumi, S., Watanabe, H., Suda, M., Tokudome, Y., Otsuka, M., Takayama, K., 2010. Infrared spectroscopic study of lipid interaction in stratum corneum treated with transdermal absorption enhancers. *Int. J. Pharm.* 389, 18–23.
- Patravale, V.B., Mandawgade, S.D., 2008. Novel cosmetic delivery systems: an application update. *Int. J. Cosmet. Sci.* 30, 19–33.
- Resch, G.P., Brandstetter, M., Königsmaier, L., Urban, E., Pickl-Herk, A.M., 2011. Immersion freezing of suspended particles and cells for cryo-electron microscopy. *Cold Spring Harb. Protoc.*, doi:10.1101/pdb.prot5642.
- Rodríguez, G., Rubio, L., Cocera, M., Estelrich, J., Pons, R., De la Maza, A., López, O., 2010. Application of bicellar systems on skin: diffusion and molecular organization effects. *Langmuir* 26, 10578–10584.
- Schwarz, J.C., Kählig, H., Matsko, N.B., Kratzel, M., Husa, M., Valenta, C., 2011. Decrease of liposomal size and retarding effect on fluconazole skin permeation by lysine derivatives. *J. Pharm. Sci.* 100, 2911–2919.
- Trotta, M., Pattarino, F., Ignoni, T., 2002. Stability of drug-carrier emulsions containing phosphatidylcholine mixtures. *Eur. J. Pharm. Biopharm.* 53, 203–208.
- Vrignaud, S., Anton, N., Gayet, P., Benoit, J.P., Saulnier, P., 2011. Reverse micelle-loaded lipid nanocarriers: a novel drug delivery system for the sustained release of doxorubicin hydrochloride. *Eur. J. Pharm. Biopharm.*, doi:10.1016/j.ejpb.2011.02.015.
- Watkinson, R.M., Herkenne, C., Guy, R.H., Hadgraft, J., Oliveira, G., Lane, M.E., 2009. Influence of ethanol on the solubility, ionization and permeation characteristics of ibuprofen in silicone and human skin. *Skin Pharmacol. Physiol.* 22, 15–21.
- Yilmaz, E., Borchert, H.H., 2005. Design of a phytosphingosine-containing, positively-charged nanoemulsion as a colloidal carrier system for dermal application of ceramides. *Eur. J. Pharm. Biopharm.* 60, 91–98.